

Kronecker PCA Based Robust SAR STAP

Kristjan Greenewald, *Student Member, IEEE*, Edmund Zelnio, and Alfred Hero III, *Fellow, IEEE*

Abstract—In this work the detection of moving targets in multiantenna SAR is considered. As a high resolution radar imaging modality, SAR detects and identifies stationary targets very well, giving it an advantage over classical GMTI radars. Moving target detection is more challenging due to the “burying” of moving targets in the clutter and is often achieved using space-time adaptive processing (STAP) (based on learning filters from the spatio-temporal clutter covariance) to remove the stationary clutter and enhance the moving targets. In this work, it is noted that in addition to the oft noted low rank structure, the clutter covariance is also naturally in the form of a space vs time Kronecker product with low rank factors. A low-rank KronPCA covariance estimation algorithm is proposed to exploit this structure, and a separable clutter cancellation filter based on the Kronecker covariance estimate is proposed. Together, these provide orders of magnitude reduction in the number of training samples required, as well as improved robustness to corruption of the training data, e.g. due to outliers and moving targets. Theoretical properties of the proposed estimation algorithm are derived and the significant reductions in training complexity are established under the spherically invariant random vector model (SIRV). Finally, an extension of this approach incorporating multipass data (change detection) is presented. Simulation results and experiments using the real Gotcha SAR GMTI challenge dataset are presented that confirm the advantages of our approach relative to existing techniques.

I. INTRODUCTION

The detection (and tracking) of moving objects in a scene is an important task for scene understanding, as motion often indicates human related activity [1]. In radar imagery, object motion causes phase changes due to the Doppler effect that can be used to identify motion in the scene. Synthetic Aperture Radar (SAR) is particularly attractive for this task as it can be used for high resolution surveillance of very large areas regardless of atmospheric conditions. In this work, we focus on the problem of detecting ground based moving objects in airborne SAR imagery, also known as SAR GMTI (SAR Ground Moving Target Indication).

Classically, moving target detection with radar has been performed using MTI radars [1], [2], which use a low carrier frequency and high pulse repetition frequency in order to detect Doppler shifts directly. This approach has significant downsides, however, including very low spatial resolution, small imaging field of view, and the inability to detect stationary targets due to minimum detectable velocity limitations. The latter issue in particular means that objects that move, stop, and then move are often lost by the tracker.

SAR, on the other hand, typically has extremely high spatial resolution (both range and cross range) and can be used to image very large areas (e.g. multiple square miles in the Gotcha data collection). As a result, stationary and slowly moving objects are easily detected and located [2], [1]. SAR GMTI is complicated by several phenomena, however. In particular, Doppler causes smearing and azimuth displacement of moving objects [3], [1] making them difficult to detect in stationary clutter, especially since the amount of smearing grows with integration time (number of pulses) [3]. Several methods have thus been developed for detecting and potentially refocusing moving targets in clutter.

SAR systems are either single channel (standard single antenna system) or multichannel. Standard approaches for the single channel scenario include autofocus [4] and velocity filters. Autofocusing, however, only works in low clutter since otherwise it will focus the clutter instead of the moving target [4], [1]. Velocity filterbank (i.e. track before detect) approaches (e.g. [3]) involve searching in a massive velocity/acceleration space, which often makes the computational complexity excessively high [1]. Attempts to reduce the computational complexity via techniques such as the compressive sensing based dictionary approach of [5] and the Bayesian inference based approach of [1] have been presented, but remain computationally intensive [1].

SAR systems often are designed to have multiple channels, one of the potential benefits of which is the potential for improved moving target detection performance [2], [1], [6]. Standard multiple channel configurations include arraying spatially separated antenna over space (multichannel SAR/STAP etc.), flying multiple passes (change detection), using multiple polarizations, or combinations thereof [1]. Downsides to these approaches include the higher data rate created by collecting multiple channels and the fact that multiple passes involve long delays, registration issues, and having to fly the same orbit more than once [1].

A. Previous Multichannel Approaches

Several techniques exist for using multiple radar channels (antennas) to separate the moving targets from the stationary background. One set of techniques involves an antenna configuration such that each antenna transmits and receives from approximately the same location but at slightly different times. We call this SAR GMTI. Along track interferometry (ATI) and displaced phase center array (DPCA) are two classical approaches for detecting moving targets in SAR GMTI data, both of which are applicable only to the two channel scenario. Both ATI and DPCA first form a SAR image for each of the antennas. To detect the moving targets, ATI thresholds the phase difference between the images (and is thus better at

K. Greenewald and A. Hero III are with the Department of Electrical Engineering and Computer Science, University of Michigan, Ann Arbor, MI, USA. E. Zelnio is with the Air Force Research Laboratory, Wright Patterson Air Force Base, OH 45433, USA. This research was partially supported by grants from AFOSR FA8650-07-D-1220-0006 and ARO MURI W911NF-11-1-0391. Approved for public release, PA Approval #88ABW-2014-6099.

canceling bright clutter) and DPCA thresholds the amplitude of the difference (and is thus better at canceling dim clutter). A Bayesian approach which used a parametric cross channel covariance generalizing ATI/DPCA to p channels (as part of a more advanced model) was developed in [1]. Space-time Adaptive Processing (STAP) uses a spatio-temporal covariance (which must be learned from training data) to model the relationships across both channels and pulses, effectively canceling the clutter [2], [6]. Using classical covariance estimation techniques (sample covariance, low rank covariance estimation) STAP requires large amounts of guaranteed target-free training data be available due to the high dimensionality of the spatio-temporal vector. In this data rich case, STAP performs significantly better than other methods [1], [2], [6]. However, with p and q the number of antennas and number of time samples (pulses), respectively, the dimension pq of the covariance is very large. Therefore, the number of degrees of freedom ($pq(pq + 1)/2$) in the covariance matrix can greatly exceed the number n of training samples available to estimate the covariance matrix. This so-called “small n large p ” problem leads to severe instability and overfitting errors.

A second set of techniques uses a coherent antenna array for which each antenna receives a delayed version of the same signal, with the array designed (e.g. a linear array) such that returns from different angles create different phase differences across the antennas ([6], [7], [8], [9] etc.). In this case, the covariance-based STAP approach, described above, can be applied to cancel the clutter [7], [6], [9].

In this paper, we focus on covariance-based STAP due to its computational efficiency and excellent clutter cancellation capabilities.

Many covariance regularization approaches exist for STAP to account for the “small n large p ” problem. None of these methods, however, specifically exploit the fact that the STAP covariance matrix has spatio-temporal structure. The contribution of this paper is to apply covariance estimation techniques designed to exploit spatio-temporal structure in order to significantly reduce the number n of training samples required as well as to provide a degree of robustness to corrupted training data.

Let q be the number of pulses and p the number of channels. Define the array $\mathbf{X}^{(m)} \in \mathbb{C}^{p \times q}$ such that $X_{ij}^{(m)}$ is the radar return from the j th pulse of the i th channel in the m th range bin. Let $\mathbf{x}_m = \text{vec}(\mathbf{X}^{(m)})$. Define

$$\Sigma = \text{Cov}(\mathbf{x}). \quad (1)$$

Radar data is complex valued and has zero mean.

The training samples used to estimate the SAR covariance are collected from n adjacent range bins. As noted above, the number of degrees of freedom in the covariance matrix can greatly exceed the number $n = |\mathcal{S}|$ (\mathcal{S} being the set of training samples) of training samples (range bins) available to estimate the covariance matrix. This is particularly the case since the covariance Σ is not constant over all range bins and over the SAR coherent processing intervals, limiting the number of available training samples. Hence, the standard

sample covariance matrix (SCM),

$$\mathbf{S} = \frac{1}{n} \sum_{m \in \mathcal{S}} \mathbf{x}_m \mathbf{x}_m^H, \quad (2)$$

may be rank deficient or ill-conditioned [1], [6], [10], [11]. Specifically, it can be shown that using the SCM directly for STAP requires a number n of training samples that is at least twice the dimension pq [12].

By introducing structure and/or sparsity into the covariance matrix, thus reducing the number of parameters to be estimated, the sampling requirements can be reduced. It has been noted [13], [6], [2] that the spatiotemporal clutter covariance Σ is very low rank in general, indicating that the clutter lives in a spatiotemporal subspace that occupies a small portion of the overall pq dimensional space. Hence, a common approach to STAP clutter cancellation [6], [7], [1] is to estimate a low rank clutter subspace from \mathbf{S} and project it away from the data. This low rank structure significantly reduces the number of parameters from order $O(p^2q^2)$ to order $O(rpq)$ where r is the dimension of the subspace. Hence, using this dimensionality reduction approach, the required number of training samples is reduced significantly [14], [6]. Efficient algorithms, including some involving subspace tracking, have been proposed [15], [16]. Additional methods have been proposed as well, such as the addition of structural constraints (e.g. persymmetry [6]), and robustification to outliers either via exploitation of the SIRV model [17] or adaptive weighting of the training data [18]. Additional fast approaches based on techniques such as Krylov subspace methods [19], [20], [21], [22] and adaptive filtering [23], [24] exist. All of these techniques are still sensitive to outlier or moving target corruption of the training data, and generally require significant training sample sizes [1]. In addition, to the best of our knowledge, none of these techniques explicitly incorporate the known spatio-temporal structure of the data into the covariance estimator.

In this paper, we exploit the explicit space-time arrangement of the covariance, by using a Kronecker product model for the clutter covariance. Specifically, the covariance matrix Σ is modeled as the Kronecker product of two smaller matrices,

$$\Sigma_c = \mathbf{A} \otimes \mathbf{B}, \quad (3)$$

where \mathbf{A} is $p \times p$ and \mathbf{B} is $q \times q$ and both \mathbf{A} and \mathbf{B} are low rank. In this setting, the \mathbf{B} matrix is the “temporal (pulse) covariance” and \mathbf{A} is the “spatial (antenna) covariance,” both determined up to a multiplicative constant. It is shown that, for the single pass case, the clutter \mathbf{A} is rank one. An extension to multipass (change detection) GMTI is also presented, for which \mathbf{A} has rank equal to the number of passes.

Kronecker product covariances arise in a variety of applications, including MIMO radar [25], geostatistics [26], recommendation systems [27], multi-task learning [28], and genomics [29]. A rich set of algorithms and associated performance guarantees exist for estimation of covariances in Kronecker product form, including iterative maximum likelihood [30], [26], noniterative L2 based approaches [30], sparsity promoting methods [26], [31], and robust ML SIRV based methods [11]. Many of these methods have been proven to achieve very significant reductions in the number of training

samples required for learning, in line with the reduction in the number of parameters [30], [26], [31].

For the SAR GMTI antenna arrangement scheme, this Kronecker model is appropriate for any spatial clutter model [1] when one assumes that antenna calibration errors are constant over the region of interest [1]. This latter condition is typically modeled as being true over reasonably large regions [1], hence sufficient training data should always be available for Kronecker covariance estimation.

In this paper, an iterative L2 based algorithm is proposed to directly estimate the low rank Kronecker factors from the observed sample covariance. Symmetric positive semidefiniteness of the estimator is proved, and theoretical performance guarantees are presented. We then introduce the Kron STAP filter, which projects away both the spatial and temporal clutter subspaces, effectively projecting away a larger subspace than does LR-STAP, thereby achieving improved noise and clutter cancelation. Due to the reduction in the number of parameters, a significant reduction in filter estimation variance is achieved.

In addition to requiring fewer training samples, it is shown that the proposed approach improves robustness to corrupted training data, critically allowing significant numbers of moving targets to remain in the training set. This is due to both the clutter and targets having Kronecker covariances with different Kronecker factors. Note that a sum of different Kronecker factors cannot be represented as a single factor model. Hence, in this sense the Kron STAP filter estimate has lower bias than unstructured LR-STAP.

To summarize, the contributions of this paper include: 1) the introduction of the low rank Kronecker product based Kron STAP filter; 2) an algorithm for estimating the spatial and temporal clutter subspaces that is highly robust to outliers due to the additional Kronecker product structure; 3) theoretical results demonstrating improved SINR sample complexity of the estimation algorithm; and 4) an extension to multipass STAP.

The remainder of the paper is organized as follows. Section II, presents the multichannel SIRV radar model, our low rank Kronecker product covariance estimation algorithm is presented in III, and our proposed STAP filter is given in Section IV. Section V discusses an extension of Kronecker STAP to the case of multiple passes (i.e. moving target change detection). Section VI gives theoretical performance guarantees and Section VII gives simulation results and the empirical results of applying our algorithms to the Gotcha dataset.

II. SIRV DATA MODEL

Let $\mathbf{X} \in \mathbb{C}^{p \times q}$ be an array of returns from an observed range bin across p channels and q pulses. As is typical [32], [7], [6], [33], we model $x = \text{vec}(\mathbf{X})$ as a spherically invariant random vector (SIRV) with the following decomposition:

$$\mathbf{x} = \mathbf{x}_{clutter} + \mathbf{x}_{noise} + \mathbf{x}_{target} \quad (4)$$

where \mathbf{x}_{noise} is Gaussian sensor noise with $\text{Cov}[\mathbf{x}_{noise}] = \sigma^2 \mathbf{I}$ and the return from the stationary clutter is given by $\mathbf{x}_{clutter} = \tau \mathbf{c}$ where τ random scalar and \mathbf{c} is a multivariate complex

Gaussian distributed vector with $\text{Cov}[\mathbf{c}] = \Sigma_c$. The signal of interest \mathbf{x}_{target} is the sum of returns from any moving targets that may be in the range bin. The mean of \mathbf{x} is zero due to the isotropic nature of radar phase noise. The resulting target free ($\mathbf{x}_{target} = 0$) covariance is given by

$$\Sigma = E[\tau] \Sigma_c + \sigma^2 \mathbf{I} \quad (5)$$

The goal of STAP is to train (from clutter range bins) a spatiotemporal filter \mathbf{F} to cancel the clutter $\mathbf{x}_{clutter}$ while preserving the moving target signals \mathbf{x}_{target} :

$$y = \mathbf{d}^H \mathbf{F} \mathbf{x} \approx \mathbf{d}^H \mathbf{x}_{target} + \mathbf{d}^H \mathbf{F} \mathbf{x}_{noise} \quad (6)$$

where \mathbf{d} is the spatio-temporal “steering vector” [6], that is, a matched filter for a specific target location/motion profile. To do this, the target and clutter signals must be in some way separable. The ideal (noiseless and stationary) return from a stationary scene in a given range bin is given by [1], [2]

$$\mathbf{x} = \mathbf{1} \otimes \mathbf{b}, \quad (7)$$

where \mathbf{b} is the ideal series of pulse returns at a single antenna, since the antennas in the radar systems under consideration are ideally located at the same points in space (though not in time). This gives a clutter covariance of

$$\Sigma_c = \mathbf{1} \mathbf{1}^T \otimes \mathbf{B}, \quad (8)$$

where

$$\mathbf{B} = E[\mathbf{b} \mathbf{b}^H]. \quad (9)$$

\mathbf{B} depends linearly on the spatial covariance function \mathbf{C} of the clutter reflectivity, which in turn depends on the spatial characteristics of the clutter in the region of interest [2]. While \mathbf{B} is not exactly low rank in general, it is approximately low rank in the sense that significant concentration in a few principal components is observed over small regions [34].

Due to the long integration time and high cross range resolution associated with SAR, the returns from the general class of moving targets are more complicated. However, if we restrict to targets with constant doppler shift within a range bin the return has the form

$$\mathbf{x} = \mathbf{a}(f) \otimes \mathbf{b}(f), \quad (10)$$

where $\mathbf{a}(f) = [1 \ e^{j2\pi\theta_1(f)} \ \dots \ e^{j\theta_p(f)}]^T$, the θ_i are proportional to the target radial velocity f and are dependent on the platform speed and antenna separation [1], and \mathbf{b} depends on the target, its Doppler shift, and its cross range path. For sufficiently large $\theta_i(f)$, $\mathbf{a}(f)^H \mathbf{1}$ will be small and the target will lie outside of the SAR clutter spatial subspace. Furthermore, as observed in [4], for long integration times the return of a moving target is significantly different from that of uniform stationary clutter, implying that moving targets generally lie outside the temporal clutter subspace [4] as well.

In practice, each antenna has gain and phase calibration errors that vary slowly across range and crossrange [1]. It was shown in [1] that these calibration errors can be modeled as constant over small regions. Let the calibration error on antenna i be $h_i e^{j\phi_i}$ and $\mathbf{h} = [h_1 e^{j\phi_1}, \dots, h_p e^{j\phi_p}]$,

giving an observed return $\mathbf{x}' = (\mathbf{h} \otimes \mathbf{I}) \odot \mathbf{x}$ and a clutter covariance of

$$\tilde{\Sigma}_c = (\mathbf{h}\mathbf{h}^H) \otimes \mathbf{B} = \mathbf{A} \otimes \mathbf{B} \quad (11)$$

A. Existing STAP Approaches

It can be shown [2], [6] that, if the clutter covariance is known, under the SIRV model the optimal (in terms of SINR when the clutter covariance is known) clutter cancellation filter is given by the whitening filter

$$\mathbf{F} = \Sigma_c^{-1}. \quad (12)$$

Traditionally, the sample covariance (2) has been used to learn the clutter covariance [6]. The sample covariance, however, has very noisy low intensity PCA components [35] when the number of training samples is on the order of the number of variables. As a result, attempting to use the pseudoinverse of the sample covariance is highly unstable and problematic. When $n \gg pq$ the inverse of the sample covariance matrix can be used to reliably estimate the optimal filter (12). However, in STAP $n \leq pq$ and a regularized inverse is often used as an approximation to (2). For this a dimensionality reduction method called clutter subspace processing is typically used.

A *clutter subspace* $\{\mathbf{u}_i\}_{i=1}^r$ is estimated using the span of the top r principal components of the clutter sample covariance [2], [6]. The corresponding clutter cancellation filter is given by the matrix \mathbf{F} that projects onto the space orthogonal to the estimated clutter subspace:

$$\mathbf{F} = \mathbf{I} - \sum_{i=1}^r \mathbf{u}_i \mathbf{u}_i^H. \quad (13)$$

This approach is effective when the clutter subspace is of low rank $r \ll pq$. Most STAP techniques were developed for a parallel signal acquisition receiving array of antennas (for which the covariance is low rank by Brennan's rule [13]) but can also be used for the sequential signal acquisition receiving antenna system used in SAR GMTI, since the clutter covariance remains low rank [1], [2].

Since the sample covariance requires a relatively large number of training samples, obtaining sufficient target free training samples that are close enough in range to be applicable is a practical problem [1], [6]. In addition, if low amplitude moving targets are accidentally included in training, the learned covariance will be corrupted and partially cancel moving targets as well, which is especially problematic in online STAP implementations [1], [15]. The STAP approach discussed below mitigates these problems as it directly takes advantage of the inherent space vs. time Kronecker structure of the clutter covariance.

III. KRONECKER SUBSPACE ESTIMATION

For the Kronecker product SIRV plus noise clutter/noise covariance model of (5), an iterative shrinkage maximum likelihood estimation algorithm was presented in [11]. While this algorithm has excellent performance in the low sample regime, it does not provide a low rank approximation. To be applicable to STAP, such an approximation is essential in order to identify

the clutter subspace. In this paper we propose a subspace estimation algorithm with low computational complexity.

Following the approach of [30], [10], [36], [11], we fit the low rank Kronecker product model (11) to the sample covariance matrix \mathbf{S} with $\text{rank}(\mathbf{A}) = r_a, \text{rank}(\mathbf{B}) = r_b$. The estimation of the parameters \mathbf{A}, \mathbf{B} in (11) is performed by minimizing the following objective function

$$\min_{\text{rank}(\hat{\mathbf{A}})=r_a, \text{rank}(\hat{\mathbf{B}})=r_b} \|\mathbf{S} - \hat{\mathbf{A}} \otimes \hat{\mathbf{B}}\|_F^2. \quad (14)$$

This objective function is not convex, however alternating minimization between \mathbf{A} and \mathbf{B} gives monotone convergence of (34) due to the nonnegativity of the objective [37]. By way of notation, for a $pq \times pq$ matrix \mathbf{M} define $\{\mathbf{M}(i, j)\}_{i,j=1}^p$ to be its $q \times q$ block submatrices, i.e. $\mathbf{M}(i, j) = [\mathbf{M}]_{(i-1)q+1:iq, (j-1)q+1:jq}$. Also, let $\bar{\mathbf{M}} = \mathbf{K}_{p,q}^T \mathbf{M} \mathbf{K}_{p,q}$ where $\mathbf{K}_{p,q}$ is the $pq \times pq$ permutation operator such that $\mathbf{K}_{p,q} \text{vec}(\mathbf{N}) = \text{vec}(\mathbf{N}^T)$ for any $p \times q$ matrix \mathbf{N} .

The alternating minimization algorithm is derived in Appendix A and given by Algorithm 1, where $\text{SVD}_r(\mathbf{M})$ denotes the matrix obtained by truncated \mathbf{M} to its first r principal components. The matrices \mathbf{A} and \mathbf{B} are only identifiable up to a scale factor. Therefore, in practice it may be advantageous to renormalize them after each iteration so that, for example, $\|\mathbf{A}\|_F = 1$. We call Algorithm 1 low rank Kronecker product covariance estimation, or LR-Kron. Furthermore, in Appendix A it is shown that when the initialization is positive semidefinite Hermitian the LR-Kron estimator $\hat{\mathbf{A}} \otimes \hat{\mathbf{B}}$ is positive semidefinite Hermitian and is thus a valid covariance matrix.

Algorithm 1 LR-Kron Covariance Estimation

- 1: $\mathbf{S} = \Sigma_{SCM}$, form $\mathbf{S}(i, j), \bar{\mathbf{S}}(i, j)$.
 - 2: Initialize \mathbf{A} s.t. $\|\mathbf{A}\|_F = 1$ (or correspondingly \mathbf{B}).
 - 3: **while** Objective (34) not converged **do**
 - 4: $\mathbf{R}_B = \frac{\sum_{i,j} a_{ij}^* \bar{\mathbf{S}}(i, j)}{\|\mathbf{A}\|_F^2}$
 - 5: $\mathbf{B} = \text{SVD}_{r_b}(\mathbf{R}_B)$
 - 6: $\mathbf{R}_A = \frac{\sum_{i,j} b_{ij} \mathbf{S}(i, j)}{\|\mathbf{B}\|_F^2}$
 - 7: $\mathbf{A} = \text{SVD}_{r_a}(\mathbf{R}_A)$
 - 8: **end while**
 - 9: **return** \mathbf{A}, \mathbf{B} .
-

IV. KRONECKER STAP

A. Filters

Once the low rank Kronecker clutter covariance has been estimated using Algorithm 1, it remains to identify a filter \mathbf{F} , analogous to (13), that uses the Kronecker covariance model. If we restrict ourselves to subspace projection filters and make the common assumption that the target component in (4) is orthogonal to the clutter subspace, then the optimal approach in terms of SINR is to project away the clutter subspace, along with any other subspaces in which targets are guaranteed not to exist. If only target orthogonality to the joint spatio-temporal clutter subspace is assumed, then the optimal STAP filter is the projection matrix:

$$\mathbf{F} = \mathbf{I} - \mathbf{U}_A \mathbf{U}_A^H \otimes \mathbf{U}_B \mathbf{U}_B^H, \quad (15)$$

where $\mathbf{U}_A, \mathbf{U}_B$ are orthogonal bases for the rank r_a and r_b subspaces of the low rank estimates of \mathbf{A} and \mathbf{B} , respectively, obtained by applying Algorithm 1. This is the Kronecker product equivalent of the standard STAP projector (13).

Additional information is available, however. Specifically, according to (10), no moving target should lie in the same spatial subspace as the clutter. This suggests the spatial only filter (which we call spatial-only Kronecker STAP)

$$\mathbf{F} = (\mathbf{I} - \mathbf{U}_A \mathbf{U}_A^H) \otimes \mathbf{I}. \quad (16)$$

to cancel as much of the clutter “subspace leakage” as possible while minimizing target cancellation. This leakage is due to noise, covariance estimation errors, and data nonidealities. Furthermore, as noted in Section II if the dimension of the clutter temporal subspace is sufficiently small relative to the dimension of the entire space, moving targets must have temporal factors (b) that lie outside of the temporal clutter subspace. Under these assumptions, it is thus MSE optimal to project away both the temporal and spatial clutter subspaces. This suggests the following form of the STAP filter \mathbf{F} :

$$\mathbf{F} = (\mathbf{I} - \mathbf{U}_A \mathbf{U}_A^H) \otimes (\mathbf{I} - \mathbf{U}_B \mathbf{U}_B^H) = \mathbf{F}_A \otimes \mathbf{F}_B. \quad (17)$$

This projects the signal x onto a $(p-1)(q-r_b)$ dimensional subspace, which is significantly smaller than the $pq - r_b$ dimensional subspace onto which (15) and unstructured STAP project the data. As a result, much more of the clutter that “leaks” outside the primary subspace can be canceled, thus allowing lower amplitude moving targets to be detected. We call the filter of (17) Kronecker STAP (KronSTAP).

B. Robustness Benefits

Besides the benefits of increasing the size of the canceled subspace while reducing the number of parameters, Kronecker STAP enjoys several other benefits arising from associated properties of (17) described below.

The clutter covariance model (11) is low rank, motivating the PCA singular value thresholding approach of classical STAP. This approach, however, is problematic in the Kronecker case because of the way low rank Kronecker factors combine. Specifically, the Kronecker product $\mathbf{A} \otimes \mathbf{B}$ has the SVD [?]

$$\mathbf{A} \otimes \mathbf{B} = (\mathbf{U}_B \otimes \mathbf{U}_B)(\mathbf{S}_A \otimes \mathbf{S}_B)(\mathbf{U}_A^H \otimes \mathbf{U}_B^H) \quad (18)$$

where $\mathbf{A} = \mathbf{U}_A \mathbf{S}_A \mathbf{U}_A^H$ and $\mathbf{B} = \mathbf{U}_B \mathbf{S}_B \mathbf{U}_B^H$ are the SVDs of \mathbf{A} and \mathbf{B} respectively. The singular values are $s_A^{(i)} s_B^{(j)}$, $\forall i, j$. As a result, a simple thresholding of singular values is not equivalent to separate thresholding of the singular values of \mathbf{A} and \mathbf{B} and hence won’t necessarily adhere to the space vs. time structure.

Now, suppose that the covariance is corrupted by the addition of a set of w rank one subspaces.

$$\mathbf{\Sigma} = \mathbf{A} \otimes \mathbf{B} + \sum_{i=1}^w \lambda_i \mathbf{u}_i \mathbf{v}_i^H \quad (19)$$

This occurs, for example, when the training data includes some sparse moving targets, since each creates a rank one signal.

The Kronecker form of the first (signal subspace) additive term on the right hand side of (19) endows the Kronecker STAP with superior clutter rejection than the standard PCA method, which is known to be vulnerable to leakage of moving target energy into the clutter subspace [1], [6]. This is because the product structure of the Kronecker clutter subspace is unlikely to be shared by moving targets.

V. MULTIPASS STAP

In surveillance applications, it is often of interest to determine what, if anything, has changed in a scene between a reference time t_0 and a later time t_1 , e.g. disappearance/appearance of parked vehicles, or the appearance of vehicle footprints [1], [14], [38], [39]. When SAR is used for “change detection” the radar platform will generally fly past the scene and form a “reference” image at time t_0 , and then at time $t_1 > t_0$ fly a path as close as possible to the original and form a new “mission” image. These images are then compared and changes detected. However, moving targets will almost always be detected as changes, along with the changes in the stationary scene background [1]. When changes of background are of primary interest, moving targets may in fact mask changes in the stationary scene due to displacement and smearing. Hence, it is advantageous to identify moving targets in both scenes prior or parallel to background change detection. In addition, it may be of interest to detect moving targets in the imagery for their own sake [1]. We thus exploit the additional scene information arising from having two images to better estimate the clutter subspace, and follow STAP with subsequent noncoherent change detection.

Our Kronecker STAP based change detection approach is as follows. The spatial channels of both registered phase histories (\mathbf{X}_k) are concatenated, forming a “ $2p$ channel phase history”

$$\mathbf{X} = \begin{bmatrix} \mathbf{X}_1 \\ \mathbf{X}_2 \end{bmatrix} \in \mathbb{C}^{2p \times q} \quad (20)$$

Since two images are involved with potentially different calibration errors, the clutter subspace is of rank 2. Thus, a rank 2 spatial clutter subspace and a low rank temporal subspace are estimated using LRKron and projected away via the KronSTAP filter. This two pass procedure is easily extended to handle multiple (> 2) passes of the radar sensor.

VI. SINR ANALYSIS

Let the STAP filter be \mathbf{F} . Then at steering vector \mathbf{d} the filter is $\mathbf{w} = \mathbf{F}\mathbf{d}$ the filter output is

$$y = \mathbf{w}^H \mathbf{x} = \tau \mathbf{w}^H \mathbf{d} + \mathbf{w}^H \mathbf{n} \quad (21)$$

In this paper, the filter $\mathbf{w} = \mathbf{F}\mathbf{d}$ [6].

The SINR at a given steering vector \mathbf{d} [6] is thus given by

$$\text{SINR}_{out} = \frac{|\tau|^2 |\mathbf{w}^H \mathbf{d}|^2}{E[\mathbf{w}^H \mathbf{n} \mathbf{n}^H \mathbf{w}]} = \frac{|\tau|^2 |\mathbf{w}^H \mathbf{d}|^2}{\mathbf{w}^H \mathbf{\Sigma} \mathbf{w}} \quad (22)$$

Define SINR_{max} to be the optimal SINR, achieved at \mathbf{w}_{opt} .

Suppose that the clutter has covariance of the form (11). Assume that the target steering vector \mathbf{d} lies outside both the temporal and spatial clutter subspaces as per above and [6].

Suppose that LR-STAP is set to use r principal components. Suppose further that Kron STAP uses 1 spatial component and r temporal components (equivalent number).

Hence under these assumptions, the SINR achieved using LR-STAP, Kron STAP or spatial Kron STAP with infinite training samples is given by [6] $SINR_{max} = \frac{|\tau|^2}{\sigma^2}$ and achieved at \mathbf{w}_{max} .

Next, we analyze the asymptotic convergence rates under the finite sample regime. Define the SINR Loss ρ as the loss of performance when using the estimate $\hat{\mathbf{w}} = \hat{\mathbf{F}}\mathbf{d}$ as the filter instead of \mathbf{w}_{max} :

$$\rho = \frac{SINR_{out}}{SINR_{max}} \quad (23)$$

Let λ_i , $i = 1, \dots, pq$ be the singular values of Σ_c . Under the Kronecker model, we have

$$\lambda_i = s_A^{(1)} s_B^{(i)}, \quad i = 1, \dots, r_b \quad (24)$$

and $\lambda_i = 0$ for $i > q$, since \mathbf{A} only has one nonzero singular value.

Theorem VI.1 (LR-STAP SINR [6]). *For large n , the expected SINR Loss of LR-STAP is*

$$E[\rho] = 1 - \frac{1}{n} \sum_{i=1}^r \left(\frac{E[\tau] \lambda_i + \sigma^2}{E[\tau] \lambda_i} \right)^2 \quad (25)$$

which in the small σ^2 regime (typical in SAR [6]) becomes

$$E[\rho] \approx 1 - \frac{r}{n} \quad (26)$$

Under the Kronecker model we have

$$E[\rho] = 1 - \frac{1}{n} \sum_{i=1}^r \left(\frac{E[\tau] s_B^{(i)} + \frac{\sigma^2}{s_A^{(1)}}}{E[\tau] s_B^{(i)}} \right)^2 \quad (27)$$

For the spatial stage of Kron STAP, we suppose that the naive estimator

$$\hat{\mathbf{A}} = \text{SVD}_1 \left(\frac{1}{q} \sum_i \mathbf{S}(i, i) \right) = \hat{\psi} \hat{\mathbf{h}} \hat{\mathbf{h}}^H \quad (28)$$

for the spatial subspace \mathbf{h} (where $\|\mathbf{h}\|_2 = 1$ is used. This is equivalent to approximating the sample spatial covariance as rank 1. The analysis of [6] thus applies with $r = 1$, except some of the “samples” are correlated. By the Kronecker structure of the covariance it is trivial to show (for the SIRV distribution) that the worst case occurs when all the temporal correlations are all ± 1 , in which case $\frac{1}{q} \sum_i \mathbf{S}(i, i)$ reduces to an n iid sample SCM with Gaussian noise variance σ^2/q and we can directly obtain via Theorem VI.1

Theorem VI.2 (Kron STAP (spatial stage) SINR). *For large n and using the estimator (28), the expected SINR Loss of the spatial stage of Kron STAP using the estimator (28) is*

$$E[\rho_s] \leq 1 - \frac{1}{n} \left(\frac{E[\tau] \psi + \frac{\sigma^2}{q}}{E[\tau] \psi} \right)^2 \quad (29)$$

where $\psi = s_A^{(1)} \frac{\text{trace}(\mathbf{B})}{q}$. In the small σ^2 regime this becomes

$$E[\rho_s] \leq 1 - \frac{1}{n} \quad (30)$$

Since under the Kronecker model the spatial stage projects away the entire clutter subspace (and then some) and spatial Kron STAP is a special case of Kron STAP, this SINR loss lower bounds the achievable SINR loss of Kron STAP. Since by Section II in worst case clutter $r = q$, the gains of using Kron STAP can be quite significant.

Turning to the temporal stage, note that by symmetry the analog of Theorem VI.2 still applies if the temporal stage is applied first instead of the spatial stage. For the case that the temporal stage follows the spatial stage, suppose that errors occurred in estimating the spatial covariance, either due to subspace estimation error or to \mathbf{A} having a rank greater than one due to small calibration errors. Specifically, suppose the estimated spatial subspace is $\tilde{\mathbf{h}}$. Then it is shown in Appendix B that the SINR Loss of the temporal Kron STAP stage is given by:

Theorem VI.3 (Kron STAP (temporal stage) SINR). *Suppose that a value for the spatial subspace estimate $\tilde{\mathbf{h}}$ used by the spatial stage of Kron STAP is fixed. Then for large n and targets with constant Doppler over the integration interval, the SINR loss from the temporal stage of Kron STAP (following the spatial stage of Kron STAP) is*

$$E[\rho_t|\tilde{\mathbf{h}}] = 1 - \frac{1}{n} \sum_{i=1}^{r_b} \left(\frac{E[\tau] s_B^{(i)} + \frac{\sigma^2}{\tilde{\mathbf{h}}^H \mathbf{A} \tilde{\mathbf{h}}}}{E[\tau] s_B^{(i)}} \right)^2 \quad (31)$$

which in the small σ^2 regime becomes

$$E[\rho_t|\tilde{\mathbf{h}}] \approx 1 - \frac{r_b}{n} \quad (32)$$

Note that in the $n \gg p$ regime relevant when $q \gg p$, $\tilde{\mathbf{h}} \approx \mathbf{h}$ (where \mathbf{h} is the first singular vector of \mathbf{A}), giving $\tilde{\mathbf{h}}^H \mathbf{A} \tilde{\mathbf{h}} \approx s_A^{(1)}$, which corresponds to the noise term in Theorem VI.1. Since $r_b \ll q$ (otherwise the moving targets will be canceled) and r_b can be smaller than $\text{rank}(\mathbf{B})$ (since in the ideal large sample regime all the clutter is removed by the temporal stage), this slower convergence rate on a smaller amount of cancellation than the spatial stage is still faster than that of LR-STAP in general.

VII. RESULTS

A. Dataset

For evaluation of our detection methods, we use the public release Gotcha SAR GMTI dataset. This dataset consists of two SAR passes through a circular path around a small scene containing various moving and stationary civilian vehicles. For image formation we use the backprojection algorithm with Blackman-Harris windowing as in [1]. For our experiments, we use 31 seconds of data, divided into 1 second (2171 pulse) coherent integration intervals.

In order to evaluate target detection performance, ground truth for all targets in the Gotcha imagery is required, but does not currently exist for the real Gotcha dataset due to the complicated displacement and smearing behavior in the

SAR imagery. Hence, for the real data we rely on non ROC measures of performance, and resort to synthetically generated data to show ROC performance gains. The real data experiments that reference example targets are based on higher amplitude targets in the dataset that we ground truthed by comparing and analyzing the results of the best detection methods available.

B. Simulations

In this section, we generate synthetic clutter plus additive noise range bins using a low rank Kronecker covariance. The covariance we use to generate the synthetic clutter via the SIRV model was learned from a set of example range bins extracted from the Gotcha dataset. We use $p = 3$, $q = 150$, $r_b = 20$, and $r_a = 1$. Spatio-temporal Kron STAP, Spatial Kron STAP, and LR-STAP are then used to learn clutter cancellation filters from the training clutter data. The mean squared residual (as a function of the number of training range bins) after then applying these filters to a set of testing clutter data is shown in Figure 1, which illustrates the $n = 1$ convergence of Kron STAP and the much slower convergence rate of unstructured LR-STAP. The MSE does not go to zero with increasing training sample size due to the noise added at testing.

Next, we consider the case that the clutter spatial covariance \mathbf{A} has a second singular value that is $1/30^2$ that of the primary instead of having only one singular value as in the ideal case. This is to illustrate small potential nonidealities and varying antenna calibration errors. The STAP algorithms remain the same with $r_a = 1$ (otherwise only a rank one potential target subspace would remain), and synthetic range bins containing both clutter and a moving target are also used in testing. The maximal filtering response over all possible steering vectors is used as a detection statistic, giving ROC curves. The AUC of these curves is plotted on the left in Figure 2 as a function of the number of training samples. Note again the poor performance and slow convergence of LR-STAP, and the superiority of the proposed spatio-temporal Kron STAP relative to Spatial Kron STAP. Spatio-temporal Kron STAP converges very quickly to the optimal Spatial Kron STAP performance, and then more slowly converges to a superior performance as the temporal filter converges. A similar plot for the case of a weaker target with the filtering response from the known target steering vector used as the detection statistic is shown on the right side of Figure 2.

Finally, the case of 5% of the training data having synthetic moving targets with random Doppler shifts is shown in Figure 3 for both the MSE and AUC experiments. As predicted above, the Kronecker methods remain largely unaffected, whereas significant losses in sample complexity are sustained by LR-STAP. This confirms the superior robustness of imposing Kronecker structure on the covariance.

C. STAP

In this subsection, STAP is applied to the Gotcha dataset mentioned above. Since the goal of SAR GMTI is target localization [2], [1], we consider steering vectors \mathbf{d}_i for each

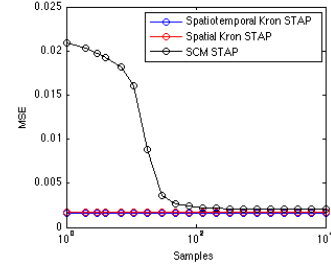


Fig. 1. Average MSE, as a function of the number of training samples, of noisy synthetic clutter filtered by spatio-temporal Kron STAP, spatial only Kron STAP, and unstructured LR-STAP filters. Note the rapid convergence and low MSE of the Kronecker methods.

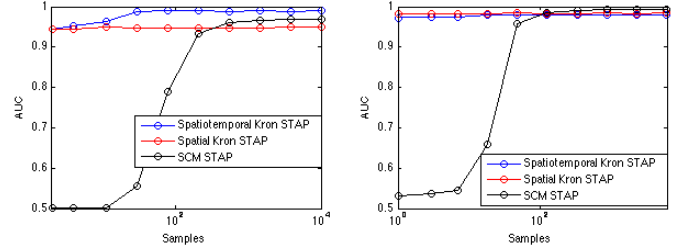


Fig. 2. Left: AUCs for detecting a synthetic target using the maximum steering vector, when slight spatial nonidealities exist in the true clutter covariance. Right: AUCs for detecting a weaker target using the true steering vector. Note the rapid convergence of the Kronecker methods, and the superior performance of spatio-temporal Kron STAP to spatial only Kron STAP.

range bin and 150 cross range pixels. In single antenna SAR imagery, each cross range pixel is a Doppler frequency bin that corresponds to the cross range location for stationary targets with that Doppler frequency as well as any overlaid moving targets. Let \mathbf{D} be the matrix of steering vectors for all 150 Doppler (cross range) bins in each range bin. Then the SAR images at each antenna are given by $\tilde{\mathbf{x}} = \mathbf{I} \otimes \mathbf{D}^H \mathbf{x}$ and the STAP output for a spatial steering vector \mathbf{h} and temporal steering \mathbf{d}_i (separable as noted in (10)) is the scalar

$$y_i(\mathbf{h}) = (\mathbf{h} \otimes \mathbf{d}_i)^H \mathbf{F} \mathbf{x} \quad (33)$$

Due to the high dimensionality involved, plots for all possible values of \mathbf{h} and i cannot be shown. Hence, for interpretability we produce images where for each range bin the i th pixel is

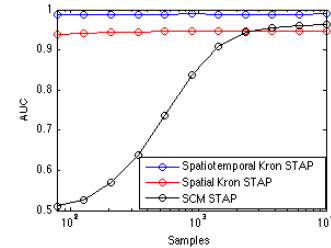


Fig. 3. AUCs for detecting a synthetic target using the maximum steering vector when (in addition to the spatial nonidealities) 5% of the training range bins contain targets with random location and velocity in addition to clutter. Note that relative to Figure 2 (left) LR-STAP has degraded significantly, whereas the Kronecker methods have not.

set as $\max_{\mathbf{h}} |y_i(\mathbf{h})|$. More sophisticated detection techniques could invoke priors on reasonable \mathbf{h} , but we leave this for future work.

Shown in Figure 7 are results for several exemplar SAR frames, showing for each example the original SAR (single antenna) image, the results of spatio-temporal Kronecker STAP, the results of Kronecker STAP with spatial filter only, the amount of enhancement (smoothed dB difference between STAP image and original) at each pixel of the spatial only Kronecker STAP, standard unstructured STAP with $r = 25$ (similar rank to Kronecker covariance estimate), and standard unstructured STAP with $r = 40$. Note the significantly improved contrast of Kronecker STAP (relative to the unstructured methods) between moving targets (example high amplitude moving targets marked in red) and the background. Additionally, note that both spatial and temporal filtering achieve significant gains. Due to the lower dimensionality, LR-STAP performs better for the image with fewer pulses, but still remains inferior to the Kronecker methods. However, the inclusion of additional pulses seems to improve target contrast for the Kronecker methods, and the additional smearing can be exploited using techniques such as shear averaging [4] which we do not consider here.

To analyze the convergence behavior of the different STAP methods, a Monte Carlo simulation was conducted where random subsets of the (bright object free) available training set were used to learn the covariance and the corresponding STAP filters. The filters were then used on each of the 31 SAR images and the MSE between the results and the STAP results learned using the entire training set were computed. The results are shown in Figure 4. Note the rapid convergence of the Kronecker methods relative to the SCM based method, as expected. This confirms that significantly fewer training samples are required under the proposed Kronecker clutter covariance model.

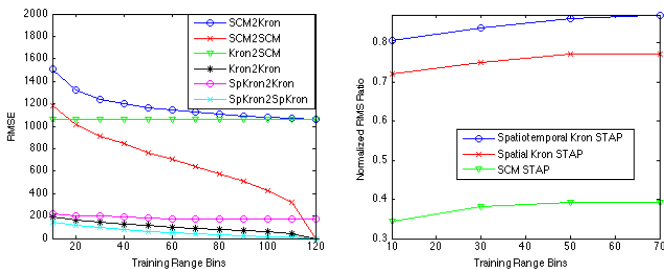


Fig. 4. Left: Average RMSE of the output of the Kronecker, spatial only Kronecker, and unstructured STAP filters relative to each method's maximum training sample output. Note the rapid convergence and low RMSE of the Kronecker methods. Right: Normalized ratio of the RMS magnitude of the brightest pixels in each target relative to the RMS value of the background, for the output of each of Kronecker STAP, spatial Kronecker STAP, and unstructured STAP.

Figure 4 (right) shows the normalized ratio of the RMS magnitude of the 10 brightest $y_i(\mathbf{h})$ for each ground truthed target to the RMS value of the background, computed for each of the STAP methods as a function of the number of training samples. This measure is large when the contrast of the target to the background is high. The Kronecker methods clearly

dominate the SCM, particularly in the low sample regime.

D. Multipass Kron STAP

Representative two pass Kronecker STAP results are shown in Figure 5, comparing to two pass LR-STAP and to standard (gain calibrated) incoherent change detection. For the STAP methods, noncoherent change detection is performed following filtering by reforming each image (via maximum steering vectors as in the previous section) and subtracting the resulting pixel magnitudes. It can be seen that additional clutter cancellation capabilities can be gained by using Kronecker STAP on multiple passes.

As in the single pass case, Figure 6 shows relative RMSE convergence results and the normalized RMS ratio between targets and background. Again, Kron STAP outperforms the other methods, and both STAP methods outperform standard incoherent change detection.

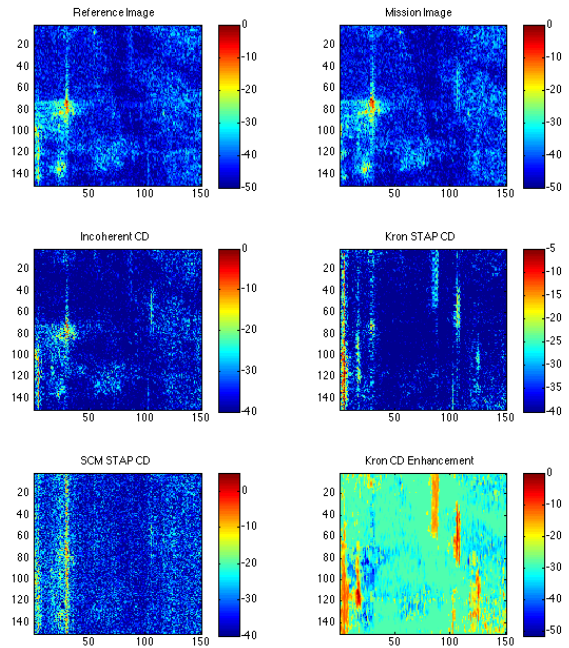


Fig. 5. Multipass STAP. An example reference and mission image pair are shown, both of which include moving targets. Shown are the results of incoherent change detection, multipass spatio-temporal Kron STAP, multipass LR-STAP, and the multipass spatial Kron STAP enhancement. Note the superior moving target enhancement of the Kronecker methods.

VIII. CONCLUSION

In this paper, we proposed a new method for clutter rejection in high resolution multiple antenna synthetic aperture radar systems for detecting moving targets. Stationary clutter signals in multichannel single-pass radar were shown to have Kronecker product structure where the spatial factor is rank one and the temporal factor is low rank. Exploitation of this structure was achieved using the Low Rank KronPCA

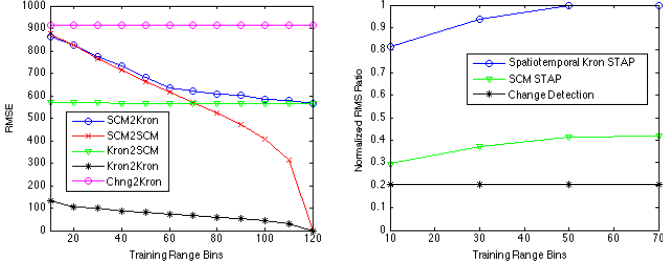


Fig. 6. Left: Average RMSE of the output of the Kronecker and unstructured STAP filters and incoherent change detection relative to each method's maximum training sample output. Note the rapid convergence and low RMSE of the Kronecker methods. Right: Normalized ratio of the RMS magnitude of the brightest pixels in each target relative to the RMS value of the background, for the output of each of Kronecker STAP, incoherent change detection, and unstructured STAP.

covariance estimation algorithm, and a new clutter cancellation filter exploiting the space-time separability of the covariance was proposed. The resulting clutter covariance estimates were applied to STAP clutter cancellation, exhibiting significant detection performance gains relative to existing low rank covariance estimation techniques. These gains were observed in both the number of training samples required and in enhanced robustness to corrupted training data. These gains were analytically characterized using a SIRV based analysis and experimentally confirmed using simulations and the Gotcha SAR GMTI dataset.

An extension of the KronSTAP approach to multi-pass SAR for moving target change detection. Significant performance gains were achieved relative to standard change detection methods.

APPENDIX A DERIVATION OF ALGORITHM 1

We have the following objective function:

$$\min_{\text{rank}(\hat{\mathbf{A}})=r_a, \text{rank}(\hat{\mathbf{B}})=r_b} \|\mathbf{S} - \hat{\mathbf{A}} \otimes \hat{\mathbf{B}}\|_F^2, \quad (34)$$

To derive the alternating minimization algorithm, fix \mathbf{B} (symmetric) and minimize (34) over low rank \mathbf{A} :

$$\begin{aligned} & \arg \min_{\text{rank}(\hat{\mathbf{A}})=r_a} \|\mathbf{S} - \hat{\mathbf{A}} \otimes \hat{\mathbf{B}}\|_F^2 \quad (35) \\ &= \arg \min_{\text{rank}(\hat{\mathbf{A}})=r_a} \sum_{i,j}^q \|\mathbf{S}(i,j) - b_{ij} \hat{\mathbf{A}}\|_F^2 \\ &= \arg \min_{\text{rank}(\hat{\mathbf{A}})=r_a} \sum_{i,j}^q |b_{ij}|^2 \|\mathbf{A}\|_F^2 - 2\text{Re}[b_{ij} \langle \mathbf{A}, \mathbf{S}^*(i,j) \rangle] \\ &= \arg \min_{\text{rank}(\hat{\mathbf{A}})=r_a} \|\mathbf{A}\|_F^2 - 2\text{Re} \left[\left\langle \mathbf{A}, \frac{\sum_{i,j}^q b_{ij} \mathbf{S}^*(i,j)}{\|\mathbf{B}\|_F^2} \right\rangle \right] \\ &= \arg \min_{\text{rank}(\hat{\mathbf{A}})=r_a} \left\| \mathbf{A} - \frac{\sum_{i,j}^q b_{ij}^* \mathbf{S}(i,j)}{\|\mathbf{B}\|_F^2} \right\|_F^2 \end{aligned}$$

where b_{ij} is the i, j th element of $\hat{\mathbf{B}}$ and b^* denotes the complex conjugate of b . This can be solved by the SVD via the Eckardt-

Young theorem. Let

$$\mathbf{R}_A = \frac{\sum_{i,j}^q b_{ij}^* \mathbf{S}(i,j)}{\|\mathbf{B}\|_F^2} \quad (36)$$

and $\mathbf{u}_i, \sigma_i, \mathbf{v}_i = \mathbf{u}_i$ be the associated SVD. The right and left singular vectors are equal because \mathbf{R}_A is positive semidefinite Hermitian if \mathbf{B} is [30]. Hence the minimizer of the objective is

$$\hat{\mathbf{A}}(\mathbf{B}) = \text{SVD}_{r_a}(\mathbf{R}_A) = \sum_{i=1}^{r_a} \sigma_i \mathbf{u}_i \mathbf{u}_i^H \quad (37)$$

Similarly minimizing \mathbf{B} with fixed positive semidefinite Hermitian \mathbf{A} gives

$$\hat{\mathbf{B}}(\mathbf{A}) = \text{SVD}_{r_b}(\mathbf{R}_B) = \sum_{i=1}^{r_b} \mathbf{u}_i \sigma_i \mathbf{u}_i^H \quad (38)$$

where now \mathbf{u}_i, σ_i describes the SVD of

$$\mathbf{R}_B = \frac{\sum_{i,j}^p a_{ij}^* \tilde{\mathbf{S}}(i,j)}{\|\mathbf{A}\|_F^2} \quad (39)$$

Iterating between the two minimizations completes the algorithm.

By induction, initializing with either a positive semidefinite Hermitian \mathbf{A} or \mathbf{B} and iterating until convergence will converge to a positive semidefinite Hermitian matrix (thus being a valid covariance matrix) since the set of positive semidefinite Hermitian matrices is closed.

APPENDIX B PROOF OF THEOREM VI.3

After the spatial stage of Kron STAP projects away (16) the estimated spatial subspace $\tilde{\mathbf{h}}$ (where $\|\tilde{\mathbf{h}}\|_2 = 1$) the remaining clutter has a covariance given by

$$((\mathbf{I} - \tilde{\mathbf{h}}\tilde{\mathbf{h}}^H)\mathbf{A}) \otimes \mathbf{B}. \quad (40)$$

By (10), the steering vector for a (constant Doppler) moving target is of the form $\mathbf{d} = \mathbf{d}_A \otimes \mathbf{d}_B$. Hence, the filtered output is

$$\begin{aligned} y &= \mathbf{w}^H \mathbf{x} = \mathbf{d}^H \mathbf{F} \mathbf{x} \quad (41) \\ &= (\mathbf{d}_A^H \otimes \mathbf{d}_B^H) (\mathbf{F}_A \otimes \mathbf{F}_B) \mathbf{x} \\ &= ((\mathbf{d}_A^H \mathbf{F}_A) \otimes (\mathbf{d}_B^H \mathbf{F}_B)) \mathbf{x} \\ &= \mathbf{d}_B^H \mathbf{F}_B \left((\mathbf{d}_A^H (\mathbf{I} - \tilde{\mathbf{h}}\tilde{\mathbf{h}}^H)) \otimes \mathbf{I} \right) \mathbf{x} \end{aligned}$$

Let $\tilde{\mathbf{d}}_A = (\mathbf{I} - \tilde{\mathbf{h}}\tilde{\mathbf{h}}^H)\mathbf{d}_A$ and define $\tilde{\mathbf{c}} = (\tilde{\mathbf{d}}_A^H \otimes \mathbf{I}) \mathbf{c}$. Then

$$y = \mathbf{d}_B^H \mathbf{F}_B (\tau \tilde{\mathbf{c}} + \tilde{\mathbf{n}}) \quad (42)$$

where $\tilde{\mathbf{n}} = (\tilde{\mathbf{d}}_A \otimes \mathbf{I}) \mathbf{n}$ and

$$\begin{aligned} \text{Cov}[\tilde{\mathbf{c}}] &= (\tilde{\mathbf{d}}_A^H \mathbf{A} \tilde{\mathbf{d}}_A) \mathbf{B} \quad (43) \\ \text{Cov}[\tilde{\mathbf{n}}] &= \sigma^2 \mathbf{I} \end{aligned}$$

which are proportional to \mathbf{B} and \mathbf{I} respectively. The scalar $(\tilde{\mathbf{d}}_A^H \mathbf{A} \tilde{\mathbf{d}}_A)$ is small if \mathbf{A} is accurately estimated, hence improving the SINR but not affecting the SINR loss. Thus, the temporal stage of Kron STAP is equivalent to single

channel LR-STAP with clutter covariance $(\tilde{\mathbf{d}}_A^H \mathbf{A} \tilde{\mathbf{d}}_A) \mathbf{B}$ and noise variance σ^2 .

Given a fixed $\hat{\mathbf{A}} = \tilde{\mathbf{h}} \tilde{\mathbf{h}}^H$, Algorithm 1 dictates (39), (38) that

$$\mathbf{R}_B = \sum_{i,j}^p \tilde{h}_i^* \tilde{h}_j^* \tilde{\mathbf{S}}(i, j) \quad (44)$$

$$\hat{\mathbf{B}} = \text{SVD}_{r_b}(\mathbf{R}_B)$$

which is thus the low rank approximation of the sample covariance of

$$\mathbf{x}_h = \mathbf{x}_{c,h} + \mathbf{n}_h = (\tilde{\mathbf{h}} \otimes \mathbf{I})^H (\mathbf{x}_c + \mathbf{n}). \quad (45)$$

Since $\mathbf{x}_c = \tau \mathbf{c}$, $\mathbf{x}_{c,h} = \tau (\tilde{\mathbf{h}} \otimes \mathbf{I})^H \mathbf{c}$ so $(\tilde{\mathbf{h}} \otimes \mathbf{I})^H \mathbf{c}$ is Gaussian with covariance

$$\text{Cov}[\mathbf{x}_{c,h}] = (\tilde{\mathbf{h}}^H \mathbf{A} \tilde{\mathbf{h}}) \mathbf{B} \quad (46)$$

and $\mathbf{x}_{c,h}$ is an SIRV. Furthermore, $\mathbf{n}_h = (\tilde{\mathbf{h}} \otimes \mathbf{I})^H \mathbf{n}$ which is Gaussian with covariance $\sigma^2 \mathbf{I}$. Thus, in both training and filtering the temporal stage of Kron STAP is exactly equivalent to single channel LR STAP. Thus to prove Theorem VI.3 it is straightforward to apply the analysis in the proof of Theorem VI.1 [6].

REFERENCES

- [1] G. E. Newstadt, E. G. Zelnio, and A. O. Hero III, "Moving target inference with hierarchical bayesian models in synthetic aperture radar imagery," *arXiv preprint arXiv:1302.4680*, 2013.
- [2] J. H. Ender, "Space-time processing for multichannel synthetic aperture radar," *Electronics & Communication Engineering Journal* **11**(1), pp. 29–38, 1999.
- [3] J. K. Jao, "Theory of synthetic aperture radar imaging of a moving target," *Geoscience and Remote Sensing, IEEE Transactions on* **39**(9), pp. 1984–1992, 2001.
- [4] J. R. Fienup, "Detecting moving targets in sar imagery by focusing," *Aerospace and Electronic Systems, IEEE Transactions on* **37**(3), pp. 794–809, 2001.
- [5] A. S. Khwaja and J. Ma, "Applications of compressed sensing for sar moving-target velocity estimation and image compression," *Instrumentation and Measurement, IEEE Transactions on* **60**(8), pp. 2848–2860, 2011.
- [6] G. Ginolhac, P. Forster, F. Pascal, and J. P. Ovarlez, "Exploiting persymmetry for low-rank space time adaptive processing," *Signal Processing* **97**, pp. 242–251, 2014.
- [7] M. Rangaswamy, F. C. Lin, and K. R. Gerlach, "Robust adaptive signal processing methods for heterogeneous radar clutter scenarios," *Signal Processing* **84**(9), pp. 1653 – 1665, 2004. Special Section on New Trends and Findings in Antenna Array Processing for Radar.
- [8] I. Kirsteins and D. Tufts, "Adaptive detection using low rank approximation to a data matrix," *Aerospace and Electronic Systems, IEEE Transactions on* **30**, pp. 55–67, Jan 1994.
- [9] A. Haimovich, "The eigencanceller: adaptive radar by eigenanalysis methods," *Aerospace and Electronic Systems, IEEE Transactions on* **32**, pp. 532–542, April 1996.
- [10] K. Greenewald, T. Tsiligkaridis, and A. Hero, "Kronecker sum decompositions of space-time data," in *Proceedings of IEEE CAMSAP*, 2013.
- [11] K. Greenewald and A. Hero, "Regularized block toeplitz covariance matrix estimation via kronecker product expansions," in *Proceedings of IEEE SSP*, 2014.
- [12] I. Reed, J. Mallett, and L. Brennan, "Rapid convergence rate in adaptive arrays," *Aerospace and Electronic Systems, IEEE Transactions on* **AES-10**, pp. 853–863, Nov 1974.
- [13] L. Brennan and F. Staudaher, "Subclutter visibility demonstration," Tech. Rep. RL-TR-92-21, Adaptive Sensors Incorporated, 1992.
- [14] Y. Bazi, L. Bruzzone, and F. Melgani, "An unsupervised approach based on the generalized gaussian model to automatic change detection in multitemporal sar images," *Geoscience and Remote Sensing, IEEE Transactions on* **43**(4), pp. 874–887, 2005.
- [15] H. Belkacemi and S. Marcos, "Fast iterative subspace algorithms for airborne stap radar," *EURASIP Journal on Advances in Signal Processing* **2006**, 2006.
- [16] M. Shen, D. Zhu, and Z. Zhu, "Reduced-rank space-time adaptive processing using a modified projection approximation subspace tracking deflation approach," *Radar, Sonar Navigation, IET* **3**, pp. 93–100, February 2009.
- [17] G. Ginolhac, P. Forster, J. P. Ovarlez, and F. Pascal, "Spatio-temporal adaptive detector in non-homogeneous and low-rank clutter," in *Acoustics, Speech and Signal Processing, 2009. ICASSP 2009. IEEE International Conference on*, pp. 2045–2048, IEEE, 2009.
- [18] K. Gerlach and M. Picciolo, "Robust, reduced rank, loaded reiterative median cascaded canceller," *Aerospace and Electronic Systems, IEEE Transactions on* **47**, pp. 15–25, January 2011.
- [19] J. Goldstein, I. S. Reed, and L. Scharf, "A multistage representation of the wiener filter based on orthogonal projections," *Information Theory, IEEE Transactions on* **44**, pp. 2943–2959, Nov 1998.
- [20] M. Honig and J. Goldstein, "Adaptive reduced-rank interference suppression based on the multistage wiener filter," *Communications, IEEE Transactions on* **50**, pp. 986–994, Jun 2002.
- [21] D. A. Pados, S. Batalama, G. Karystinos, and J. Matyjas, "Short-data-record adaptive detection," in *Radar Conference, 2007 IEEE*, pp. 357–361, IEEE, 2007.
- [22] L. Scharf, E. Chong, M. Zoltowski, J. Goldstein, and I. S. Reed, "Subspace expansion and the equivalence of conjugate direction and multistage wiener filters," *Signal Processing, IEEE Transactions on* **56**, pp. 5013–5019, Oct 2008.
- [23] R. Fa and R. C. De Lamare, "Reduced-rank stap algorithms using joint iterative optimization of filters," *Aerospace and Electronic Systems, IEEE Transactions on* **47**(3), pp. 1668–1684, 2011.
- [24] R. Fa, R. C. de Lamare, and L. Wang, "Reduced-rank stap schemes for airborne radar based on switched joint interpolation, decimation and filtering algorithm," *Signal Processing, IEEE Transactions on* **58**(8), pp. 4182–4194, 2010.
- [25] K. Werner and M. Jansson, "Estimation of kronecker structured channel covariances using training data," in *Proceedings of EUSIPCO*, 2007.
- [26] T. Tsiligkaridis, A. Hero, and S. Zhou, "On convergence of kronecker graphical lasso algorithms," *IEEE Trans. Signal Proc.* **61**(7), pp. 1743–1755, 2013.
- [27] G. I. Allen and R. Tibshirani, "Transposable regularized covariance models with an application to missing data imputation," *The Annals of Applied Statistics* **4**(2), pp. 764–790, 2010.
- [28] E. Bonilla, K. M. Chai, and C. Williams, "Multi-task gaussian process prediction," in *NIPS*, 2007.
- [29] J. Yin and H. Li, "Model selection and estimation in the matrix normal graphical model," *Journal of Multivariate Analysis* **107**, 2012.
- [30] K. Werner, M. Jansson, and P. Stoica, "On estimation of cov. matrices with kronecker product structure," *IEEE Trans. on Sig. Proc.* **56**(2), pp. 478–491, 2008.
- [31] S. Zhou et al., "Gemini: Graph estimation with matrix variate normal instances," *The Annals of Statistics* **42**(2), pp. 532–562, 2014.
- [32] K. Yao, "A representation theorem and its applications to spherically-invariant random processes," *Information Theory, IEEE Transactions on* **19**(5), pp. 600–608, 1973.
- [33] G. Ginolhac, P. Forster, F. Pascal, and J.-P. Ovarlez, "Performance of two low-rank stap filters in a heterogeneous noise," *Signal Processing, IEEE Transactions on* **61**, pp. 57–61, Jan 2013.
- [34] L. Borcea, T. Callaghan, and G. Papanicolaou, "Synthetic aperture radar imaging and motion estimation via robust principal component analysis," *SIAM Journal on Imaging Sciences* **6**(3), pp. 1445–1476, 2013.
- [35] B. Moore, R. Nadakutiti, and J. Fessler, "Improved robust pca using low-rank denoising with optimal singular value shrinkage," in *Proceedings of IEEE SSP*, 2014.
- [36] T. Tsiligkaridis and A. Hero, "Covariance estimation in high dimensions via kronecker product expansions," *IEEE Trans. on Sig. Proc.* **61**(21), pp. 5347–5360, 2013.
- [37] S. Boyd and L. Vandenberghe, *Convex optimization*, Cambridge university press, 2009.
- [38] F. Bovolo and L. Bruzzone, "A detail-preserving scale-driven approach to change detection in multitemporal sar images," *Geoscience and Remote Sensing, IEEE Transactions on* **43**(12), pp. 2963–2972, 2005.
- [39] K. I. Ranney and M. Soumekh, "Signal subspace change detection in averaged multilook sar imagery," *Geoscience and Remote Sensing, IEEE Transactions on* **44**(1), pp. 201–213, 2006.

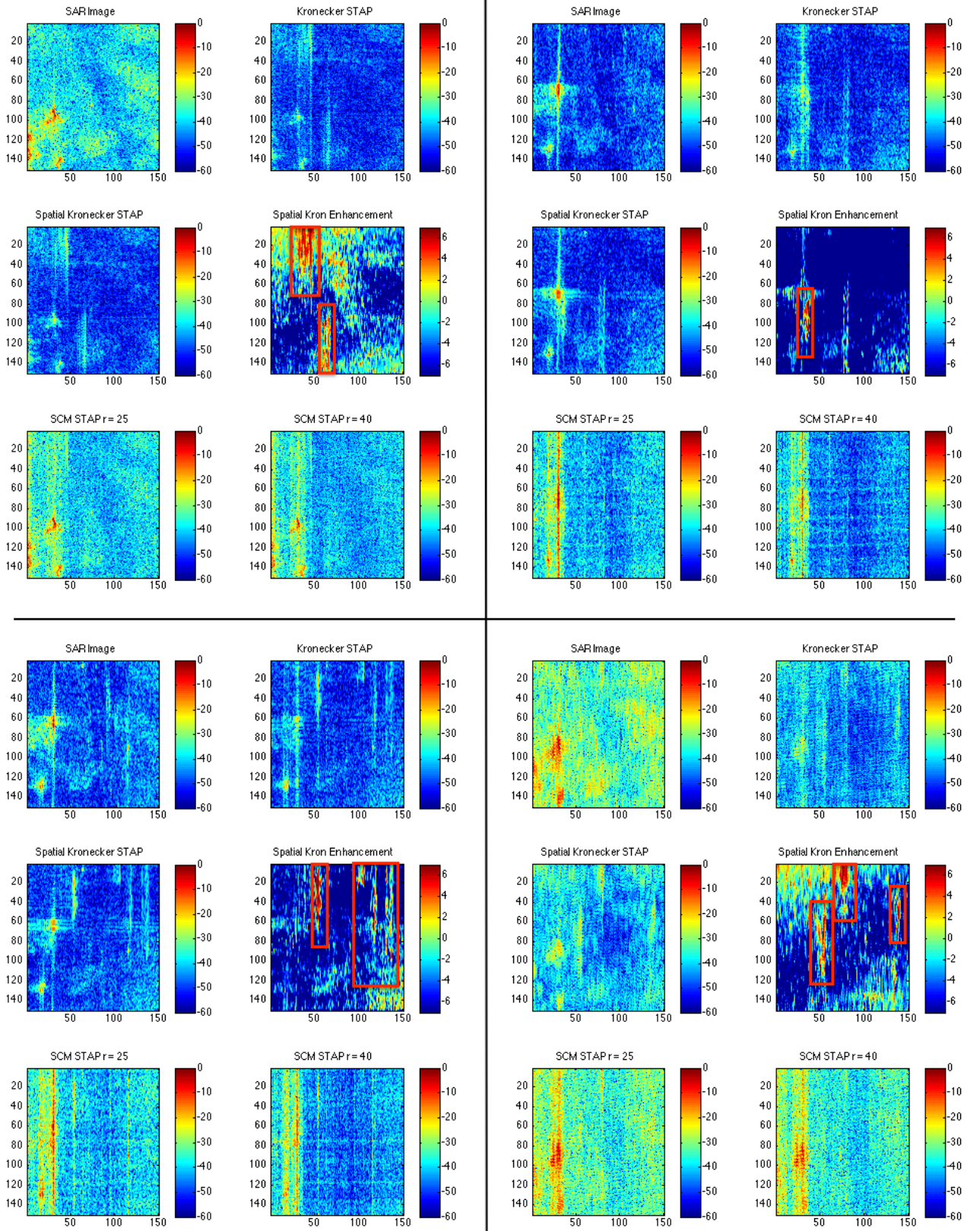


Fig. 7. Four example radar images from the Gotcha dataset along with associated STAP results. The lower right example uses 526 pulses, the remaining three use 2171 pulses. Several moving targets are highlighted in red in the spatial Kronecker enhancement plots. Note the superiority of the Kronecker methods.